

## Article

# Research on High- and Low-Temperature Rheological Properties of High-Viscosity Modified Asphalt Binder

Zhongcai Huang<sup>1</sup>, Xianwu Ling<sup>2,\*</sup>, Di Wang<sup>3</sup> , Pengfei Li<sup>2</sup>, Huaquan Li<sup>1</sup>, Xinyu Wang<sup>1</sup>, Zujian Wang<sup>1</sup>, Rong Wei<sup>1</sup>, Weining Zhu<sup>1</sup> and Augusto Cannone Falchetto<sup>3,\*</sup>

<sup>1</sup> Guangxi Communications Investment Group Corporation Ltd., Nanning 530022, China

<sup>2</sup> School of Highway, Chang'an University, Xi'an 710064, China

<sup>3</sup> Department of Civil Engineering, Aalto University, 02150 Espoo, Finland

\* Correspondence: 2021121186@chd.edu.cn (X.L.); augusto.cannonefalchetto@aalto.fi (A.C.F.)

**Abstract:** This study evaluates the critical high- and low-temperature rheological properties of a high-viscosity modified asphalt (HVMA) binder by analyzing one neat and three high-viscosity modified binders (B-type, Y-type, and H-type) using temperature sweep tests and multi-stress creep recovery tests (MSCR) through the dynamic shear rheometer (DSR), and low-temperature creep stiffness properties by the bending beam rheometer (BBR). Technical indexes such as the softening point temperature, dynamic viscosity, rutting factor, unrecoverable creep compliance, and the creep recovery rate are measured and calculated for high-temperature properties, while the m/S value, dissipation energy ratio, relaxation time, elongation, creep stiffness, and creep speed are used as technical indexes for low-temperature properties. The results show that the incorporation of high-viscosity modifiers reduces the unrecoverable creep compliance and increases the creep recovery rate of the asphalt binder. Non-recoverable creep compliance is found to be a reliable indicator for high-temperature performance, while at low temperatures, the relaxation time decreases, the dissipation energy increases, and the stress relaxation ability improves. The dissipation energy ratio and m/S value are suggested to evaluate the low-temperature performance of HVMA binders using the Burgers model based on the BBR bending creep stiffness test. Therefore, this study recommends using the unrecoverable creep compliance via MSCR to evaluate high-temperature properties and dissipation energy ratio and m/S value for low-temperature properties in the evaluation of HVMA binders.

**Keywords:** HVMA binder; rheological theory; unrecoverable creep compliance; dissipation energy ratio; m/S value



**Citation:** Huang, Z.; Ling, X.; Wang, D.; Li, P.; Li, H.; Wang, X.; Wang, Z.; Wei, R.; Zhu, W.; Falchetto, A.C. Research on High- and Low-Temperature Rheological Properties of High-Viscosity Modified Asphalt Binder. *Buildings* **2023**, *13*, 1077. <https://doi.org/10.3390/buildings13041077>

Academic Editor: Salvatore Antonio Biancardo

Received: 19 March 2023

Revised: 11 April 2023

Accepted: 18 April 2023

Published: 19 April 2023



**Copyright:** © 2023 by the authors. Licensee MDPI, Basel, Switzerland. This article is an open access article distributed under the terms and conditions of the Creative Commons Attribution (CC BY) license (<https://creativecommons.org/licenses/by/4.0/>).

## 1. Introduction

With the advancement of pavement materials and mixtures capable of meeting specific performance under different temperatures, deformations, and functions, higher and higher requirements are put forward for the creation of modified asphalt materials such as SBS, rubber, and high viscosity modified binders by increasing the amount of asphalt binder in the mix [1–4]. Because modified asphalt material can improve the road performance requirements of asphalt binders, it is widely used in road engineering. Among them, high-viscosity modified asphalt (HVMA) binders refer to a modified material with a viscosity higher than 20,000 Pa·s at 60 °C [5–7]. Because of its excellent bonding force and strong adhesion to aggregates, it can be used as one of the future recycling mixtures [8–10] and has been widely adopted in porous asphalt mixtures [11], stress absorption layers [12], bridge deck pavement layers [13] and other domains [14–16].

The main areas of research on HVMA in recent years have been the making of modified asphalt, the performance of modified asphalt at high and low temperatures, and its use as a binder in pavement materials. More investigation has conducted additional research on the rheological characteristics of HVMA binders, particularly high-temperature responses.

Chen et al., investigated the effects of high-viscosity modifier (HVM) content on the characteristics of modified binders and contrasted it with neat asphalt using 60 °C viscosity as the key indicator. The findings demonstrated that high-viscosity modified materials were quite compatible with a neat bituminous binder at 60 °C [17]. Li et al., used vacuum decomposition capillary and dynamic shear rate scanning experiments to examine the capillary viscosity and zero shear viscosity of a HVM binder. The findings demonstrate that the viscosity characteristics of high-viscosity asphalt binders vary depending on the state they are in, and for those with viscosities greater than 30,000 Pa·s, zero shear viscosity can be used to characterize the material's bonding properties [18]. Tan et al., created HVMA by modifying matrix asphalt with thermoplastic elastomer and SBS particles. The effectiveness was then compared to engineering high-viscosity asphalt, SBS-modified asphalt, and 70 # asphalt. The findings revealed that the modified materials dispersed well in asphalt and that the TPE particles, which function as high-elastic interlocking units, were spread uniformly throughout the network structure. The T-HVA also displayed better high-temperature stability and low-temperature flexibility [19]. PG high temperature grading, multi-stress repeated creep, accelerated fatigue, temperature scanning, and other procedures were used by Li et al., to set up HVMA for use in high-temperature environments. They compared and analyzed the alterations of the high temperature, fatigue resistance, and shear resistance indexes. The study's findings are beneficial for the development of porous asphalt mixtures and their use in high-temperature regions [20]. Yu et al., developed waste-LDPE/SBS composites to produce environmentally beneficial HVMA. The rheological properties and microstructure of asphalt were examined using a DSR, BBR, and fluorescence imaging. The findings demonstrate that waste polymers can significantly increase the performance of asphalt at high temperatures and lengthen the fatigue life of asphalt materials [21]. Using a DSR, Guo et al., examined the dynamic viscoelastic characteristics of a high viscosity, high elasticity, high strength, and SBS-modified glue. The results showed that different kinds of modified asphalt binders performed differently at high temperatures depending on their equilibrium complex shear modulus [22]. The rheological characteristics of three different types of high-viscosity changed materials were examined using DSR by Qin et al., who also compared them to the neat binder. It was discovered that HVMA binders had superior thermal stability and deformation recovery ability at high temps compared to the neat binder [23]. By using a BBR, Zhang et al., investigated the low-temperature rheological characteristics of neat asphalt and high-viscosity modified binders (BBR). The findings show that the production of the HVMA binder with a plasticizer and crosslinking agent can enhance its low-temperature performance [24]. Zhang et al., used macro and micro tests, including BBR and FTIR, to examine the efficacy of HVMA. The findings demonstrate a relationship between the structural properties of the compounds and the thermal properties of asphalt for the HVMA binder's low-temperature rheological properties [25].

Researchers have studied the high- and low-temperature rheological properties of high-viscosity modified binders over time, and on the basis of their findings [26–28], they have proposed the assessment index of high-temperature rheological properties of HVMA binders. Among them, most of the rheological properties of high-viscosity modified asphalt are similar to those of neat asphalt, such as complex shear modulus,  $m/S$  value and rutting factor. Still, the research needs to reach a deeper level, considering specific indicators and expanding the limited analysis of low-temperature rheological properties of high-viscosity modified materials. As a result, it is essential to research the crucial high- and low-temperature rheological characteristics of HVMA binders. In order to methodically investigate these characteristics, the DSR and the BBR experiments were performed on three different types of high-viscosity modified binders. To find more useful high- and low-temperature performance key evaluation indexes for HVMA binders and to establish a foundation for judging the caliber of high-viscosity modified binders, seven high-temperature performance evaluation indexes and six low-temperature performance evaluation indexes were chosen for a differentiation analysis.

## 2. Raw Materials and Test Methods

### 2.1. Asphalt Material

The neat material was the SK-90 road asphalt binder, and two commercially available high-viscosity modifiers (B-type and Y-type) were selected. The thermoplastic rubber that makes up the high-viscosity modifier is mixed with granular modifiers such as adhesive resin, plasticizer, and anti-aging substance. Compared with the Y-type high viscosity modifier, the B-type high viscosity modifier also added a small amount of carbon black. The main physical indexes are depicted in Table 1. The HVMA binders were made by adding HVM to the neat material. The neat asphalt binder was melted into a flowing state during the preparation process, and the high-viscosity modifier was then applied at a temperature of 170–180 °C (the content was 12% of the mass of the neat binder [23]). After operating at moderate speed (2000 r/min) for 10 min, the high speed (5000 r/min) was maintained for 30 min. To remove the bubbles created during the shearing procedure, it was put in an oven at 175 °C for 10 min after shearing was finished. For comparison, the study also selected a completed high-viscosity modified binder (H-type). Table 2 displays the key characteristics for the four various bitumen binders.

**Table 1.** Physical indexes of the high-viscosity modifier.

Test Item	Test Value	Index
Particle Size/mm	4.5	≤5
Density/(g/cm <sup>3</sup> )	0.8	0.7~1.0
Water Absorption/%	0.4	<1%

**Table 2.** Characteristics of asphalt binders.

Type	Penetration (25 °C, 5 s, 100 g)/(0.1 mm)	Softening Point/°C	Ductility (5 °C)/cm	Dynamic Viscosity (60 °C)/(Pa·s)
SK-90	97.1	47.4	9.7	140.3
B-type	51.1	84.3	64.3	38,696.9
Y-type	54.6	85.9	59.9	20,425.1
H-type	49.3	94.2	48.6	99,635.4

### 2.2. Test Method

The DSR test can be used to gauge the viscosity and elastic characteristics of asphalt binders. In the study, temperature sweep test and MSCR test of HVMA binders were used to investigate the high temperature rheological properties. HVMA binders' low temperature creep stiffness properties were investigated using a BBR test.

#### 2.2.1. Temperature Sweep Test

Consequently, the AASHTO T315 [29] temperature scanning tests are performed using the DSR. The measurement is conducted in the 3 °C to 80 °C temperature range using a 25 mm parallel plate with a 1 mm gap. Then, the step size is 5 °C, and the angular frequency is 10 rad/s.

#### 2.2.2. MSCR Test [30]

A DSR was used to conduct the test, which involved shear creep and recovery at two different stress levels at a predetermined temperature. First, 0.1 kPa and 3.2 kPa were the two creep stress values that were applied. At the 0.1 kPa stress level, twenty cycles were run. Then, for a total runtime of 300 s, ten cycles at the 3.2 kPa stress level were performed. Each cycle was further split into a 1 s stress loading stage and a 9 s zero stress recovery stage [31,32]. Considering the actual reference pavement conditions [33], the test temperature was imposed to be 64 °C. The asphalt binder specimens were short-term aged and tested with the 8 mm plate and 2 mm gap. MSCR test uses the non-recoverable creep

compliance  $J_{nr}$  and the creep recovery rate  $R$  as the evaluation index, and the calculation formula is shown in Equations (1) and (2).

$$J_{nr} = \frac{\varepsilon_u}{\sigma} \quad (1)$$

$$R = \frac{\varepsilon_p - \varepsilon_u}{\varepsilon_p} \times 100\% \quad (2)$$

above  $\varepsilon_p$  is the peak strain;  $\varepsilon_u$  is the unrecovered strain; and  $\sigma$  is the stress.

### 2.2.3. BBR Test

The BBR test measures the stiffness and relaxation performance of the asphalt binder at low temperatures. The BBR test was employed in this study to assess the asphalt's low temperature rheological characteristics. The measurement temperature was set to  $-12\text{ }^\circ\text{C}$ ,  $-18\text{ }^\circ\text{C}$ , and  $-24\text{ }^\circ\text{C}$  in accordance with AASHTO T313 [34] requirements.

## 3. Test Results and Analysis

### 3.1. High-Temperature Rheological Properties

#### 3.1.1. Rutting Factor

The variation of the rutting factor ( $G^* / \sin(\delta)$ ) with the temperature for SK-90, B-type, Y-type, and H-type is shown in Figure 1. The  $G^* / \sin(\delta)$  of the four different types of asphalt binders diminishes as the temperature rises, suggesting that the resistance to rutting will decrease as well. Then, the  $G^* / \sin(\delta)$  of B-type, Y-type and H-type HVMA binders were greater than those of the neat binder, indicating that adding a high-viscosity modifier greatly improved the rutting resistance of the neat binder. In the process of high temperature to low temperature, the anti-rutting ability of HVMA binders is better and better than that of the neat binder, indicating that the high temperature rheological properties of high viscosity asphalt should be selected under high temperature conditions. Based on field data [33], it was noted that asphalt pavement could become as hot as  $65\text{ }^\circ\text{C}$  in the summer, so the  $G^* / \sin(\delta)$  at  $65\text{ }^\circ\text{C}$  was chosen as the evaluation index of high-viscosity modified binders. The  $G^* / \sin(\delta)$  of the three HVMA binders at  $65\text{ }^\circ\text{C}$  were 15,519 Pa (B-type), 10,964 Pa (Y-type) and 19,921 Pa (H-type), respectively. The order from large to small is H-type > B-type > Y-type, indicating that an H-type high-viscosity modified binder has the best rutting resistance.

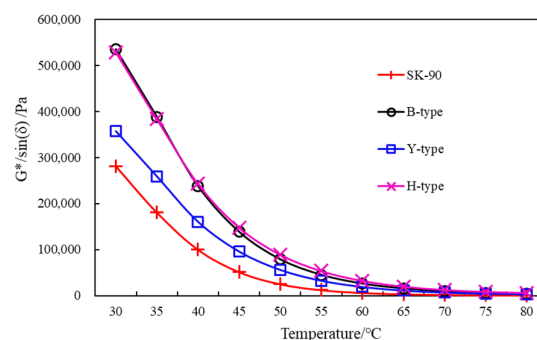


**Figure 1.** Rutting factor evolution with temperature.

#### 3.1.2. Non-Recoverable Creep Compliance and Creep Recovery Rate

Figure 2 shows the above MSCR test results at  $64\text{ }^\circ\text{C}$ . Figure 2 shows that under multiple stress loads, the time–strain curve of SK-90 is greater than those of the three HVMA binders. This pattern shows that the neat binder's high-temperature rheological properties can be greatly enhanced by high-viscosity modifiers. Comparing the time–strain curves of the three high-viscosity modified binders, it is evident that the time–strain curve of H-type is the lowest (the best high-temperature rheological properties). In contrast, the

time–strain curves of B-type and Y-type are relatively similar, indicating that the difference in the high-temperature rheological properties of B-type and Y-type is insignificant. It is found that the time–strain curves of SK-90 under two stress levels are one order of magnitude smaller than those of HVMA binders under the same stress and temperature conditions, which indicates that the addition of a high-viscosity modifier greatly enhances the high-temperature deformation resistance of asphalt.

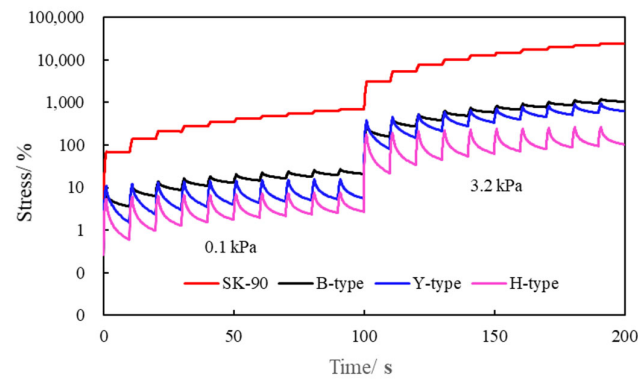


**Figure 2.** The time–strain relationship of different asphalt’s MSCR test.

The  $J_{nr}$  and  $R$  were calculated according to Equations (1) and (2). The outcomes are displayed in Figures 3 and 4. In the figure,  $J_{nr0.1}$  and  $J_{nr3.2}$  represent the average values of non-recoverable creep compliance of the binder in ten cycles under 0.1 kPa and 3.2 kPa stress, respectively.  $R_{0.1}$  and  $R_{3.2}$  represent the average values of the  $R$  of the binder in ten cycles under 0.1 kPa and 3.2 kPa stress, respectively. Figure 3 shows that the SK-90 neat, B-type, and Y-type HVMA binders all have lower levels of resistance to irreversible deformation than the H-type HVMA binder. The  $J_{nr}$  of the four binders in a high-stress level (3.2 kPa) is higher than that in a low-stress level (0.1 kPa), demonstrating that under higher stress conditions, an asphalt binder is more susceptible to permanent deformation. Figure 4 shows that under the low-stress level, the  $R$  values of H-type HVMA and Y-type high-viscosity modified binders are not much different and greater than that of B-type high-viscosity modified and SK-90 neat asphalt binders. Under the high-stress level, the  $R$  of the four types of asphalt binders from the largest to the smallest is H-type, Y-type, B-type, and SK-90. Compared to the  $R$  value under the low-stress level,  $R$  under the high-stress level has different degrees of reduction. Among them, the B-type high-viscosity modified material has the most significant decrease, reaching 15%, and a minimal 0.9% decrease in the H-type HVMA binder.

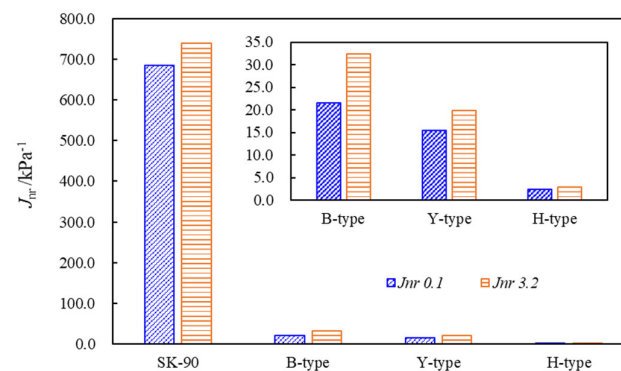


**Figure 3.** Unrecoverable creep compliance of different asphalt binders.

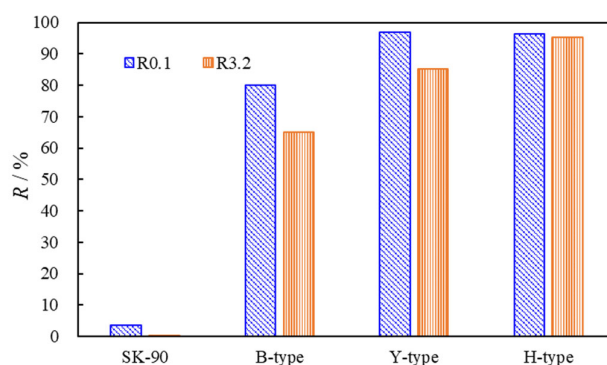


**Figure 4.** Creep recovery rate of different asphalt binders.

### 3.1.3. Analysis of High-Temperature Performance Evaluation Index

For the high-temperature evaluation index of HVMA binders, relevant researchers have performed considerable work, still demanding a unified view. In order to assess the high-temperature performance of HVMA binders, it is essential to investigate an evaluation index. Table 3 lists seven different high-temperature evaluation indexes of high-viscosity modified binders, separately for Softening Point, Dynamic Viscosity,  $G^*/\sin(\delta)$ , the  $J_{nr0.1}$  and  $J_{nr3.2}$ , and the  $R0.1$  and  $R3.2$ . In this paper, the discriminating capability of high-temperature performance evaluation indexes of high-viscosity modified binders is studied using the discrimination analysis method. Discrimination analysis is a method of using an independent sample  $t$ -test to study whether there are differences in the collection of test data. Discrimination is the quantitative power of an evaluation index in distinguishing among specific characteristics; the greater the value of discrimination  $D$ , the more sensitive the index is [35]. This paper used SPSS software to calculate the discrimination of high-temperature evaluation indexes, shown in Table 4.

**Table 3.** Different evaluation indexes of high-temperature property.

Type	Softening Point/ $^{\circ}\text{C}$	Dynamic Viscosity (60 $^{\circ}\text{C}$ )/(Pa·s)	$G^*/\sin(\delta)$ (65 $^{\circ}\text{C}$ )/Pa	$J_{nr0.1}$ (64 $^{\circ}\text{C}$ )/ $\text{kPa}^{-1}$	$J_{nr3.2}$ (64 $^{\circ}\text{C}$ )/ $\text{kPa}^{-1}$	$R0.1$ (64 $^{\circ}\text{C}$ )	$R3.2$ (64 $^{\circ}\text{C}$ )
B-type	84.3	38,696.9	15,518.6	21.54	32.39	80.1	64.9
Y-type	85.9	20,425.1	10,964.2	15.47	19.9	96.9	85.1
H-type	94.2	99,635.4	19,921.1	2.41	2.9	96.2	95.2

**Table 4.** Discrimination—calculation result of high-temperature property.

Index	Softening Point/ $^{\circ}\text{C}$	Dynamic Viscosity (60 $^{\circ}\text{C}$ )/(Pa·s)	$G^*/\sin(\delta)$ (65 $^{\circ}\text{C}$ )/Pa	$J_{nr0.1}$ (64 $^{\circ}\text{C}$ )/ $\text{kPa}^{-1}$	$J_{nr3.2}$ (64 $^{\circ}\text{C}$ )/ $\text{kPa}^{-1}$	$R0.1$ (64 $^{\circ}\text{C}$ )	$R3.2$ (64 $^{\circ}\text{C}$ )
$D$	0.000061	0.134179	0.007432	0.151634	0.190717	0.000309	0.002042

Table 4 shows the ranking of the seven different kinds of high-temperature performance evaluation indexes for HVMA in terms of discrimination:  $J_{nr3.2}$  (64  $^{\circ}\text{C}$ ) >  $J_{nr0.1}$  (64  $^{\circ}\text{C}$ ) > Dynamic Viscosity (60  $^{\circ}\text{C}$ ) >  $G^*/\sin(\delta)$  (65  $^{\circ}\text{C}$ ) >  $R3.2$  (64  $^{\circ}\text{C}$ ) >  $R0.1$  (64  $^{\circ}\text{C}$ ) > Softening Point. This shows that the MSCR test can better discriminate HVMA binders. The distinguishing ability of unrecoverable creep compliance is the best. Because the softening point test is empirical, it cannot be used to assess the high-temperature performance of HVMA because it has the lowest softening point discrimination. The performance of HVMA binders at high temperatures is recommended to be assessed using the unrecoverable creep compliance of the MSCR test.

### 3.2. Low-Temperature Rheological Properties

#### 3.2.1. Burgers Model

A typical viscoelastic material is an asphalt binder. The viscoelastic properties of modified asphalt binders can be adequately described by the Burgers model. It is a four-element viscoelastic constitutive model with a series-parallel connection made of two spring elements and two dashpot elements. The mathematical equation is [36]:

$$\varepsilon(t) = \sigma_0 \left[ \frac{1}{E_1} + \frac{1}{\eta_1} t + \frac{1}{E_2} \left( 1 - e^{-\frac{E_2}{\eta_2} t} \right) \right] \quad (3)$$

In the formula,  $\varepsilon$  is strain;  $\sigma_0$  is the applied stress, MPa;  $E_1$  is instantaneous elastic modulus;  $\eta_1$  is the instantaneous viscosity coefficient;  $E_2$  is the slow deformation after applying stress; and  $\eta_2$  is a viscosity index whose deformation does not disappear immediately after the applied stress is removed.

The BBR test data of the four asphalt binders were nonlinearly fitted (by 1stOpt—First Optimization software) to identify the Burgers model parameters. The relaxation time ( $\lambda$ ) and dissipation energy ratio ( $W_d(t)/W_s(t)$ ) of the four materials were calculated by fitting parameters  $E_1$ ,  $E_2$ ,  $\eta_1$ , and  $\eta_2$ . The calculation formula is as follows [36]:

$$\lambda = \eta_1 / E_1 \quad (4)$$

$$W_d(t)/W_s(t) = \left[ \frac{t}{\eta_1} + \frac{1}{2E_2} (1 - e^{-\frac{2E_2}{\eta_2} t}) \right] / \left[ \frac{1}{E_1} + \frac{1}{2E_2} (1 - 2e^{-\frac{E_2}{\eta_2} t} + e^{-\frac{2E_2}{\eta_2} t}) \right] \quad (5)$$

where  $t$  is the stress action time, and  $s$  is the stress level.

Relaxation time reflects the measurement of the stress of the asphalt binder with time. The longer the relaxation period, the more unfavorable (slow) the stress dissipation in the asphalt binder is [37]. The evolution of the relaxation time over temperature for the four binders can be ordered using the formulas and as shown in Figure 5: SK-90, Y-type, B-type, and H-type. The H-type high-viscosity modified binder presents the shortest relaxation time, suggesting the best low-temperature performance. As the temperature decreases, the relaxation time increases; this is because at a lower temperature, the binder elasticity increases, then the viscosity effect reduces, the energy consumption rate becomes slower, and the time allowing the stress change becomes longer, resulting in longer relaxation times.

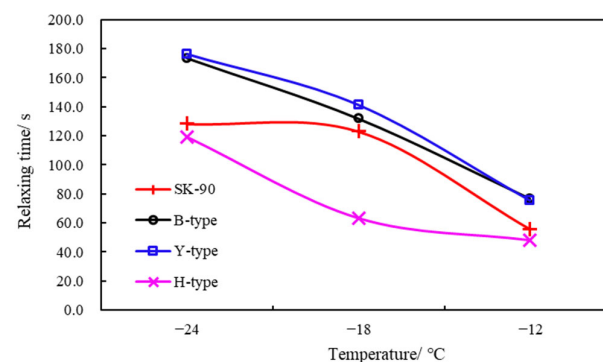


**Figure 5.** The relaxation time of asphalt binders under different temperatures.

The dissipation energy ratio shows the asphalt binder's ability to relax; the higher the dissipation energy ratio, the greater the material's low-temperature crack resistance [37]. Figure 6 presents the dissipation energy ratio for the four binders and the following trend: H-type, B-type, Y-type, and SK-90. The low-temperature performance of the H-type is the best in terms of dissipation energy, which is consistent with the relaxation time evaluation findings. The dissipation energy ratio of asphalt binders reduces as the temperature drops, demonstrating that the dissipation energy in the binders decreases, the stored

energy rises, and low-temperature crack resistance worsens. In the temperature range of  $-18\text{ }^{\circ}\text{C}\sim-12\text{ }^{\circ}\text{C}$ , the dissipation energy ratio of the four binders decreases significantly, while in the temperature range of  $-24\text{ }^{\circ}\text{C}\sim-18\text{ }^{\circ}\text{C}$ , the dissipation energy ratio of the four materials exhibits a minor reduction, indicating that as the temperature drops, the elastic ratio of the binders rises, but as the temperature drops further, the binder approaches a glassy state.

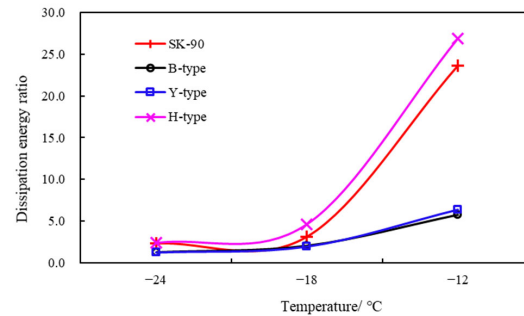


**Figure 6.** Dissipation energy ratio of the binders under different temperatures.

### 3.2.2. Creep Stiffness and Creep Speed

Figures 7 and 8 display the  $S$  and  $m$  numbers of the four binders. Low-temperature crack resistance becomes worse as the temperature lowers due to an increase in asphalt's  $S$  value. Under various low-temperature circumstances, the order of  $S$  for the four binders from large to small is SK-90, B-type, Y-type, and H-type. From the stiffness perspective, the H-type HVM binder has a better low-temperature crack resistance than SK-90, B-type, and Y-type asphalt. While the temperature decreases, the  $m$  value of asphalt increases, but there is no apparent consistency in the variation of the  $m$  value of the four binders under various temperature conditions. It can be seen that different asphalts show the same law: under low temperature conditions, the creep stiffness modulus of asphalt increases while the creep rate decreases; the creep stiffness modulus can better reflect the modulus difference between different asphalts, but, all in all, using  $S$  or  $m$  alone to assess the low-temperature performance of HVMA has obvious limitations.

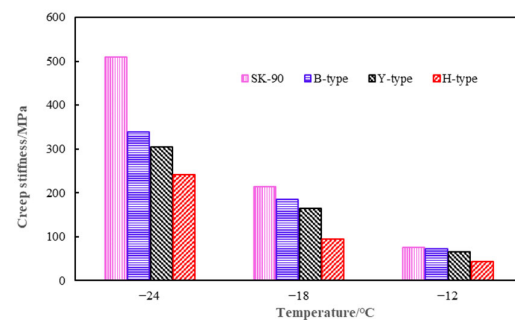


**Figure 7.** Creep stiffness of different asphalt binders.

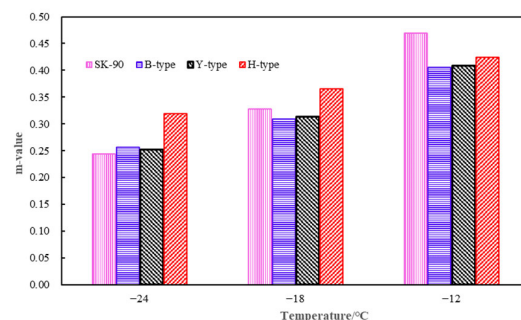


**Figure 8.**  $m$ -value of different asphalt binders.

### 3.2.3. m/S Value

According to other studies [38], the low-temperature characteristics of asphalt can be described by the m/S ratio; the higher the ratio, the better the low-temperature properties of the asphalt material. The m/S values of the four materials at various temperatures are depicted in Figure 9. The fact that the m/S values of B-type, Y-type, and H-type high-viscosity modified binders are higher than those of neat asphalt binder (SK-90) under low-temperature settings shows that high-viscosity modifiers can greatly enhance binders' low-temperature performance. Among them, the m/S value of H-type high-viscosity modified material is the highest, indicating that H-type HVMA has the greatest low-temperature performance. The increase rate of m/S value of the four materials evaluated in the temperature range of  $-24\text{ }^{\circ}\text{C}\sim-18\text{ }^{\circ}\text{C}$  is less than that in the temperature range of  $-18\text{ }^{\circ}\text{C}\sim-12\text{ }^{\circ}\text{C}$ . This trend is due to the increasing temperature leading to the higher energy of molecular motion in the binder, facilitating the activity of the molecular chain segments and structure in the material.

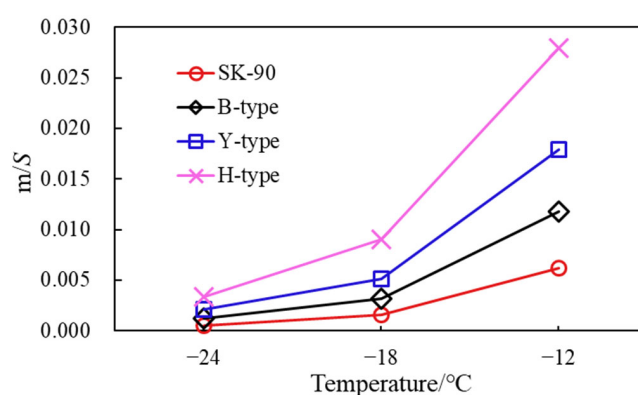


Figure 9. m/S for the different asphalt binders.

### 3.2.4. Analysis of Low-Temperature Performance Evaluation Index

Over the years, there has been limited research in identifying suitable evaluation indexes for the low-temperature performance of HVMA binders. Consequently, it is essential to investigate an evaluation index suitable for evaluating the low-temperature performance of HVMA binders. Section 3.1.3's discrimination analysis method is also used to investigate the low-temperature performance evaluation index of HVMA binders. In this paper, m/S value ( $-12\text{ }^{\circ}\text{C}$ ), ductility ( $5\text{ }^{\circ}\text{C}$ ), creep stiffness ( $-12\text{ }^{\circ}\text{C}$ ), creep speed ( $-12\text{ }^{\circ}\text{C}$ ), relaxation time ( $-12\text{ }^{\circ}\text{C}$ ), and dissipation energy ratio ( $-12\text{ }^{\circ}\text{C}$ ) are selected as different low-temperature performance evaluation indexes of HVMA binders (see Table 5). The discrimination capability of low-temperature evaluation indexes is presented in Table 6.

Table 5. Different evaluation indexes for low-temperature properties.

Type	m/S ( $-12\text{ }^{\circ}\text{C}$ )	Density/ ( $\text{g}/\text{cm}^3$ )	S ( $-12\text{ }^{\circ}\text{C}$ )/ MPa	m ( $-12\text{ }^{\circ}\text{C}$ )	$\lambda$ ( $-12\text{ }^{\circ}\text{C}$ )	$W_d(t)/W_s(t)$ ( $-12\text{ }^{\circ}\text{C}$ )
B-type	0.00556	64.3	73	0.406	76.87	5.75
Y-type	0.00617	59.9	66.2	0.409	75.30	6.34
H-type	0.01	48.6	42.4	0.424	48.30	26.86

Table 6. Discrimination capability of low-temperature evaluation indexes.

Index	m/S ( $-12\text{ }^{\circ}\text{C}$ )	Density/ ( $\text{g}/\text{cm}^3$ )	S ( $-12\text{ }^{\circ}\text{C}$ )/ MPa	m ( $-12\text{ }^{\circ}\text{C}$ )	$\lambda$ ( $-12\text{ }^{\circ}\text{C}$ )	$W_d(t)/W_s(t)$ ( $-12\text{ }^{\circ}\text{C}$ )
D	0.020454	0.001740	0.011869	0.000007	0.008249	0.407520

Table 6 demonstrates that the sequence of discrimination of low-temperature performance evaluation indexes for high-viscosity modified binders is as follows:  $W_d(t)/W_s(t)$  ( $-12\text{ }^\circ\text{C}$ ) > m/S ( $-12\text{ }^\circ\text{C}$ ) > S ( $-12\text{ }^\circ\text{C}$ ) >  $\lambda$  ( $-12\text{ }^\circ\text{C}$ ) > elongation ( $5\text{ }^\circ\text{C}$ ,  $5\text{ cm}\cdot\text{min}^{-1}$ ) > m ( $-12\text{ }^\circ\text{C}$ ). The dissipation energy ratio and m/S value have the best discrimination power. This paper recommends that the dissipation energy ratio and m/S value should be utilized to assess the low-temperature performance of a HVM binder, rather than creep stiffness or creep rate alone.

#### 4. Conclusions

Based on the results of the analysis, the following inferences can be drawn:

- (1) At  $65\text{ }^\circ\text{C}$ , the rut factor values of the three HVMA binders are all greater than 10,000 Pa, and the unrecoverable creep compliance under different stress levels is much smaller than that of neat asphalt, and the creep recovery rate is much larger than that of matrix asphalt. At a low temperature, the dissipation energy ratio and m/S value of the three kinds of HVMA binders are smaller than those of neat asphalt. These show that the use of high viscosity modifiers is positive to improve the performance of asphalt and high-viscosity modifiers can significantly enhance asphalt's high-temperature deformation resistance, significantly reduce the possibility of low-temperature crack resistance, and have good deformation recovery ability.
- (2) Considering seven high-temperature performance evaluation indexes of HVMA binders, such as rutting factor, dynamic viscosity, softening point, non-recoverable creep compliance, and creep recovery rate, it is recommended to use the MSCR test's non-recoverable creep compliance to evaluate the high-temperature performance of HVMA.
- (3) Elongation, creep stiffness, creep speed, dissipation energy ratio, and relaxation time were chosen as low-temperature performance evaluation indexes of high-viscosity modified binders. The Burgers model's dissipation energy ratio and m/S value are recommended for evaluating the low-temperature performance of high-viscosity modified materials.
- (4) This study investigates the high- and low-temperature rheological performance index of a HVMA binder and provides the recommended high and low temperature performance evaluation index. Due to the small number of asphalt samples used in the test, we will test more samples in the follow-up study to study and analyze the more accurate rheological performance index of HVMA binders, and will provide the basis for determining the quality of high-viscosity modified binders.

**Author Contributions:** Conceptualization, X.L. and Z.H.; data curation, H.L. and R.W.; formal analysis, X.W. and Z.W.; writing—review and editing, D.W.; writing—original draft, P.L.; methodology, P.L. and A.C.F.; software, D.W. and W.Z.; validation, H.L. and X.W.; investigation, Z.W.; resources, R.W. and W.Z.; visualization, Z.H.; supervision, A.C.F.; project administration, X.L. All authors have read and agreed to the published version of the manuscript.

**Funding:** This research was funded by the Scientific and Technological Development Project of Guangxi Communications Investment Group Corporation Ltd., grant number 2021-001. We would like to thank Dongdong Yuan (Chang'an University, China) for his assistance on laboratory experiments.

**Conflicts of Interest:** The authors declare no conflict of interest.

#### References

1. Wang, D.; Baliello, A.; Poulikakos, L.; Vasconcelos, K.; Kakar, M.R.; Giancontieri, G.; Pasquini, E.; Porot, L.; Tušar, M.; Riccardi, C.; et al. Rheological properties of asphalt binder modified with waste polyethylene: An interlaboratory research from the RILEM TC WMR. *Resour. Conserv. Recycl.* **2022**, *186*, 106564. [[CrossRef](#)]
2. Yuan, D.; Jiang, W.; Xiao, J.; Tong, Z.; Jia, M.; Shan, J.; Ogbon, A.W. Assessment of the aging process of finished product-modified asphalt binder and its aging mechanism. *J. Mater. Civ. Eng.* **2022**, *34*, 04022174. [[CrossRef](#)]
3. Tong, Z.; Guo, H.; Gao, J.; Wang, Z. A novel method for multi-scale carbon fiber distribution characterization in cement-based composites. *Constr. Build. Mater.* **2019**, *218*, 40–52. [[CrossRef](#)]

4. Jia, M.; Sha, A.; Jiang, W.; Li, X.; Jiao, W. Developing a solid–solid phase change heat storage asphalt pavement material and its application as functional filler for cooling asphalt pavement. *Energy Build.* **2023**, *285*, 112935. [[CrossRef](#)]
5. Sha, A.; Liu, Z.; Jiang, W.; Qi, L.; Hu, L.; Jiao, W.; Barbieri, D.M. Advances and development trends in eco-friendly pavements. *J. Road Eng.* **2021**, *1*, 1–42. [[CrossRef](#)]
6. Yuan, D.; Jiang, W.; Hou, Y.; Xiao, J.; Ling, X.; Xing, C. Fractional derivative viscoelastic response of high-viscosity modified asphalt. *Constr. Build. Mater.* **2022**, *350*, 128915. [[CrossRef](#)]
7. Cai, J.; Wen, Y.; Wang, D.; Li, R.; Zhang, J.; Pei, J.; Xie, J. Investigation on the cohesion and adhesion behavior of high-viscosity asphalt binders by bonding tensile testing apparatus. *Constr. Build. Mater.* **2020**, *261*, 120011. [[CrossRef](#)]
8. Cai, J.; Song, C.; Zhou, B.; Tian, Y.; Li, R.; Zhang, J.; Pei, J. Investigation on high-viscosity asphalt binder for permeable asphalt concrete with waste materials. *J. Clean. Prod.* **2019**, *228*, 40–51. [[CrossRef](#)]
9. Büchler, S.; Falchetto, A.C.; Walther, A.; Riccardi, C.; Wang, D.; Wistuba, M.P. Wearing Course Mixtures Prepared with High Reclaimed Asphalt Pavement Content Modified by Rejuvenators. *Transp. Res. Rec.* **2018**, *2672*, 96–106. [[CrossRef](#)]
10. Hugener, M.; Wang, D.; Cannone Falchetto, A.; Porot, L.; Kara De Maeijer, P.; Tabatabaee, E.; Kawakami, A.; Hafko, B.; Grilli, A.; Pasquini, E.; et al. Recommendation of RILEM TC 264 RAP on the evaluation of asphalt recycling agents for hot mix asphalt. *Mater. Struct.* **2022**, *55*, 31. [[CrossRef](#)]
11. Gao, J.; Yao, Y.; Yang, J.; Song, L.; Xu, J.; He, L.; Tao, W. Migration behavior of reclaimed asphalt pavement mastic during hot mixing. *J. Clean. Prod.* **2022**, *376*, 134123. [[CrossRef](#)]
12. Jiang, W.; Yuan, D.; Shan, J.; Ye, W.; Lu, H.; Sha, A. Experimental study of the performance of porous ultra-thin asphalt overlay. *Int. J. Pavement Eng.* **2022**, *23*, 2049–2061. [[CrossRef](#)]
13. Jia, M.; Sha, A.; Lin, J.; Zhang, Z.; Qi, B.; Yuan, D. Polyurethane asphalt binder: A promising candidate for steel bridge deck-paving material. *Int. J. Pavement Eng.* **2022**, *23*, 3920–3929. [[CrossRef](#)]
14. Cao, Y.; Li, J.; Sha, A.; Liu, Z.; Zhang, F.; Li, X. A power-intensive piezoelectric energy harvester with efficient load utilization for road energy collection: Design, testing, and application. *J. Clean. Prod.* **2022**, *369*, 133287. [[CrossRef](#)]
15. Yuan, D.; Jiang, W.; Sha, A.; Xiao, J.; Wu, W.; Wang, T. Technology method and functional characteristics of road thermoelectric generator system based on Seebeck effect. *Appl. Energy* **2023**, *331*, 120459. [[CrossRef](#)]
16. Xinxin, G.; Zhang, C.; Cui, B.-X.; Wang, D.; Tsai, J. Analysis of Impact of Transverse Slope on Hydroplaning Risk Level. *Procedia Soc. Behav. Sci.* **2013**, *96*, 2310–2319.
17. Chen, Y.; Tan, Y.; Chen, K. Effect of TPS modifier on the properties of high viscosity asphalt. *J. Harbin Inst. Technol.* **2012**, *44*, 82–85.
18. Li, L.; Geng, H.; Sun, Y. Evaluation method and indicator for viscosity of high-viscosity asphalt. *J. Build. Mater.* **2010**, *13*, 352–356.
19. Tan, Y.; Haiyan, Z.; Dongwei, C.; Lei, X.; Rongjie, D.; Zhaoqiang, S.; Rui, D.; Xianhe, W. Study on cohesion and adhesion of high-viscosity modified asphalt. *Int. J. Transp. Sci. Technol.* **2019**, *8*, 394–402.
20. Li, M.; Zeng, F.; Xu, R.; Cao, D.; Li, J. Study on Compatibility and Rheological Properties of High-Viscosity Modified Asphalt Prepared from Low-Grade Asphalt. *Materials* **2019**, *12*, 3776. [[CrossRef](#)]
21. Yu, H.; Jin, Y.; Liang, X.; Dong, F. Preparation of Waste-LDPE/SBS Composite High-Viscosity Modifier and Its Effect on the Rheological Properties and Microstructure of Asphalt. *Polymers* **2022**, *14*, 3848. [[CrossRef](#)] [[PubMed](#)]
22. Guo, Y.; Ni, F. Dynamic viscoelastic properties of modified asphalt and mixture based on DSR. *J. Southeast Univ.* **2014**, *44*, 386–390.
23. Qin, X.; Zhu, S.; He, X.; Jiang, Y. High temperature properties of high viscosity asphalt based on rheological methods. *Constr. Build. Mater.* **2018**, *186*, 476–483. [[CrossRef](#)]
24. Zhang, F.; Hu, C. Preparation and properties of high viscosity modified asphalt. *Polym. Compos.* **2017**, *38*, 936–946. [[CrossRef](#)]
25. Zhang, F.; Hu, C.; Zhuang, W. The research for low-temperature rheological properties and structural characteristics of high-viscosity modified asphalt. *J. Therm. Anal. Calorim.* **2018**, *131*, 1025–1034. [[CrossRef](#)]
26. Yuan, D.; Jiang, W.; Xiao, J.; Lu, H.; Wu, W. Thermal-oxygen aging effects on viscoelastic properties of high viscosity modified asphalt. *J. Chang. Univ.* **2020**, *40*, 1–11.
27. Jiang, W.; Li, P.; Sha, A.; Li, Y.; Xiao, J.; Xing, C. Research on Pavement Traffic Load State Perception Based on the Piezoelectric Effect. *IEEE Trans. Intell. Transp. Syst.* **2023**, 1–15. [[CrossRef](#)]
28. Yuan, D.; Jiang, W.; Xiao, J. Comparison of rheological properties between SBS, rubber and high-viscosity modified asphalt binders. *J. Chang. Univ.* **2020**, *40*, 135–142.
29. AASHTO T315; Determining the Rheological Properties of Asphalt Binder Using a Dynamic Shear Rheometer (DSR). AASHTO: Washington, DC, USA, 2010.
30. ASTM D7405-20; Standard Test Method for Multiple Stress Creep Recovery (MSCR) Test of Asphalt Binder Using a Dynamic Shear Rheometer. American Association of State Transport and Officials: Washington, DC, USA, 2012.
31. Tong, Z.; Gao, J.; Zhang, H. Innovation for evaluating aggregate angularity based upon 3D convolutional neural network. *Constr. Build. Mater.* **2017**, *155*, 919–929. [[CrossRef](#)]
32. Sun, Y.; Wang, W.; Chen, J. Investigating impacts of warm-mix asphalt technologies and high reclaimed asphalt pavement binder content on rutting and fatigue performance of asphalt binder through MSCR and LAS tests. *J. Clean. Prod.* **2019**, *219*, 879–893. [[CrossRef](#)]
33. Jiang, W.; Yuan, D.; Xu, S.; Hu, H.; Xiao, J.; Sha, A.; Huang, Y. Energy harvesting from asphalt pavement using thermoelectric technology. *Appl. Energy* **2017**, *205*, 941–950. [[CrossRef](#)]

34. *AASHTO T313*; Determining the Flexural Creep Stiffness of Asphalt Binder Using the Bending Beam Rheometer (BBR). AASHTO: Washington, DC, USA, 2008.
35. Wang, W.; Jia, M.; Jiang, W.; Lou, B.; Jiao, W.; Yuan, D.; Li, X.; Liu, Z. High temperature property and modification mechanism of asphalt containing waste engine oil bottom. *Constr. Build. Mater.* **2020**, *261*, 119977. [[CrossRef](#)]
36. Lin, P.; Huang, W.; Tang, N.; Xiao, F.; Li, Y. Understanding the low temperature properties of Terminal Blend hybrid asphalt through chemical and thermal analysis methods. *Constr. Build. Mater.* **2018**, *169*, 543–552. [[CrossRef](#)]
37. Wu, W.; Jiang, W.; Yuan, D.; Lu, R.; Shan, J.; Xiao, J.; Ogbon, A.W. A review of asphalt-filler interaction: Mechanisms, evaluation methods, and influencing factors. *Constr. Build. Mater.* **2021**, *299*, 124279. [[CrossRef](#)]
38. Xing, C.; Jiang, W.; Li, M.; Wang, M.; Xiao, J.; Xu, Z. Application of atomic force microscopy in bitumen materials at the nanoscale: A review. *Constr. Build. Mater.* **2022**, *342*, 128059. [[CrossRef](#)]

**Disclaimer/Publisher's Note:** The statements, opinions and data contained in all publications are solely those of the individual author(s) and contributor(s) and not of MDPI and/or the editor(s). MDPI and/or the editor(s) disclaim responsibility for any injury to people or property resulting from any ideas, methods, instructions or products referred to in the content.